

Original article

MiRNAs regulate iron homeostasis in *Paracoccidioides brasiliensis*Juliana S. de Curcio^a, Lucas Nojosa Oliveira^a, Mariana P. Batista^a, Evandro Novaes^b,
Célia Maria de Almeida Soares^{a,*}^a Laboratório de Biologia Molecular, Instituto de Ciências Biológicas, Universidade Federal de Goiás, Campus II Samambaia, CEP: 74690-900, Goiânia, Goiás, Brazil^b Departamento de Biologia, Universidade Federal de Lavras, Minas Gerais, CEP: 37200-000, Brazil

ARTICLE INFO

Article history:

Received 9 April 2020

Accepted 27 October 2020

Available online 4 November 2020

Keywords:

Paracoccidioidomycosis

RNAseq

MICRORNA

Paracoccidioides brasiliensis

IRON

ABSTRACT

During pathogen interaction with the host, several mechanisms are used to favor or inhibit the infectious process; one is called nutritional immunity, characterized by restriction of micronutrients to pathogens. Several studies on fungi of the *Paracoccidioides* complex, have demonstrated that these pathogens remodel their metabolic pathways to overcome the hostile condition imposed by the host. However, molecular mechanisms that control the regulation of those metabolic changes are not fully understood. Therefore, this work characterizes the expression profile of miRNAs during iron deprivation and describes metabolic pathways putatively regulated by those molecules. Through analysis of RNAseq, 45 miRNAs were identified and eight presented alterations in the expression profile during iron deprivation. Among the differentially regulated miRNAs, five were more abundant in yeast cells during iron deprivation and interestingly, the analyses of genes potentially regulated by those five miRNAs, pointed to metabolic pathways as oxidative phosphorylation, altered in response to iron deprivation. In addition, miRNAs with more abundance in iron presence, have as target genes encoding transcriptional factors related to iron homeostasis and uptake. Therefore, we suggest that miRNAs produced by *Paracoccidioides brasiliensis* may contribute to the adaptive responses of this fungus in iron starvation environment.

Published by Elsevier Masson SAS on behalf of Institut Pasteur.

1. Introduction

The regulation of availability of metals by host directly influence the development of the pathogen during the infectious process. Metals are micronutrients that play important roles in the host and pathogen and, during infection, both compete for them [1,2]. In this way, the host can prevent access to these metals, requiring adaptation of the pathogen to survive and promote a successful infection [3]. On the other hand, pathogens must keep metal homeostasis in order to promote a successful infection [4]. Iron is a redox-active metal and is essential as a cofactor in the form of heme and iron-sulfur clusters in a variety of cellular processes such as respiration, amino acid metabolism, peroxide detoxification, DNA replication, along with DNA and sterol biosynthesis [5,6]. For this reason, the deprivation of this metal is a condition that requires the use of alternative, non-iron dependent strategies for the maintenance of metabolism [7].

Members of the *Paracoccidioides* complex are the etiological agents of paracoccidioidomycosis (PCM), a systemic granulomatous mycosis, highly prevalent in Latin American countries [8]. Previous works described that *Paracoccidioides* spp. harbor in their genomes genes related to iron homeostasis [9]. *Paracoccidioides lutzii*, strain 01, survives to iron deprivation by inducing the expression of genes involved in energy metabolism, amino acid catabolism, vacuolar protein degradation, as well as increased pathways related to iron acquisition [10]. During *P. lutzii* infection, high concentrations of iron increase the host's susceptibility to infection [10]. To maintain iron levels, members of the *Paracoccidioides* genus depict mechanisms for the iron uptake from siderophores [11] and from heme/hemoglobin [12], as well as ferrous/ferric iron by non-classical reductive iron assimilation (RIA), which includes ferric reductases and Fe/Zn permeases [13].

Recent research has shown that members of the genus *Paracoccidioides* possess two paralogous genes coding for dicers and argonauts, important proteins in the processing of non-coding RNAs which are involved in post-transcriptional gene silencing, in the genus *Paracoccidioides* [14] as seen in other fungi. Non-coding RNAs, a class that includes miRNAs (miRNAs) are molecules

* Corresponding author.

E-mail address: cmasoares@gmail.com (C.M. de Almeida Soares).

transcribed from the genome and not translated into polypeptides. They function in regulating gene expression, both transcriptionally and post-transcriptionally. As post-transcriptional regulators of almost all biological processes, miRNAs are capable of regulating hundreds of different genes by binding to complementary sequences in the messenger RNA (mRNA), resulting in inhibition in the translation or degradation of the target mRNA [15]. Studies have shown that miRNAs influence different biological processes such as cell proliferation, apoptosis, cell differentiation, innate adaptive immune responses and the development of mycosis [16,17]. The presence of miRNAs was previously predicted by *in silico* screening in *Paracoccidioides* genomes [14] or by high performance sequencing [18].

Evidence suggests that the nutritional status of iron also plays a significant role in the function of miRNAs [19,20]. Iron and miRNAs exhibit a bidirectional relationship: the amount of iron may affect biogenesis and processing of miRNA, while miRNA contributes to the control of iron metabolism [19]. In this way, the regulation of iron homeostasis in prokaryotes is influenced by the expression of microRNAs; for example the expression of the RyhB small RNA, in *Escherichia coli* rapidly induces degradation of mRNAs, encoders of the proteins NADH dehydrogenase, iron superoxide dismutase, cytochromes, succinate dehydrogenase, among others [21]. MiRNAs produced by *Pseudomonas aeruginosa* in iron deprivation negatively regulate several targets involved with iron-dependent pathways, such as TCA, biosynthesis of Fe–S cluster proteins and sulfur metabolism [22]. MiRNAs have also been described in the control of iron metabolism in plant and animal [23]; however a similar role in fungi has not yet been elucidated.

Currently, some studies have identified the importance of miRNAs in members of the *Paracoccidioides* complex. We have demonstrated by RNAseq microRNAs regulating genes related to cell wall reorganization and energy production in mycelium and yeast forms, probably contributing to the establishment of the infection [18]. Although those descriptions the role of microRNAs in the fungus response to iron deprivation is not available, so far. Therefore, we investigated miRNAs of *Paracoccidioides brasiliensis*, expressed during *in vitro* iron deprivation, condition faced by this fungus in host. In this sense, to develop this work, libraries of small RNAs were obtained, and cDNAs were sequenced. By using bioinformatics tools, cDNAs with differential expression in yeast cells facing iron deprivation were obtained. Our results demonstrate that iron deprivation induces the expression of miRNAs, putatively controlling the expression of proteins involved with oxidative phosphorylation, response to oxidative stress and synthesis of chitin. Additionally, miRNAs with higher abundance in the iron presence may regulate transcriptional factors related to iron uptake systems. In this way, we suggest that miRNAs may contribute to the control of iron homeostasis *P. brasiliensis*.

2. Materials and methods

2.1. Microorganisms and cultures conditions

P. brasiliensis (ATCC 32069) in the yeast phase, was cultivated and maintained in Fava Netto solid medium [24], at 36 °C. After three days in solid medium, the cells were inoculated in Fava Netto's liquid medium [24] at 36 °C, under agitation (150 rpm), for 72 h. After, the cells were collected by centrifugation at 12,000×g for 10 min at 4 °C and the pellet was washed with phosphate-buffered saline (PBS 1 X). A total of 10⁶ cells/mL were inoculated in modified Mc Veigh & Morton minimal liquid medium (MMcM) [25] containing: 4% (w/v) glucose, 0.15% (w/v) KH₂PO₄, 0.05% (w/v) MgSO₄·7H₂O, 0.015% (w/v) CaCl₂·2H₂O, 0.2% (w/v) (NH₄)₂SO₄, 0.2% (w/v) L-asparagine, 0.02 (w/v) L-cystine, 1% (v/v) of vitamin

supplement [0.006% (w/v) thiamine, 0.006% (w/v) niacin B3, 0.006% (w/v) Ca⁺² pantothenate, 0.001% (w/v) inositol B7, 0.0001% (w/v) biotin B8, 0.001% (w/v) riboflavin, 0.01% (w/v) folic acid B9, 0.01% (w/v) choline chloride, 0.01% (w/v) pyridoxine] and 0.1% (v/v) of trace elements supplement [0.0057% (w/v) boric acid H₃BO₃, 0.0081% (w/v) MnSO₄ 14 H₂O, 0.0036% (w/v) (NH₄)₆ MO₇O₂₄· 4 H₂O, 0.0157% (w/v) CuSO₄·H₂O, 0.1404 (w/v) pH 7.2. MMcM medium supplemented with 3.5 μM Fe (NH₄)₂(SO₄)₂, was used as control. Iron deprivation was achieved in MMcM medium supplemented with 50 μM of bifophenanthroline bisulphonic acid (BPS) [10]. The cultures were grown under agitation at 150 rpm for 24 h at 36 °C. After, cells cultivated in iron presence or deprivation were centrifuged at 12,000×g, for 10 min; the supernatants were discarded and RNAs were obtained by using TRIzol (TRI Reagent, Sigma–Aldrich, St. Louis, MO), according to the manufacturer's instructions. The RNA samples from 24 h of cultivation in presence or iron deprivation were employed for real-time PCR and for next-generation sequencing experiments; the RNA samples were obtained in experimental triplicate.

2.2. Analysis of the integrity of RNAs, construction of small cDNA libraries, next-generation sequencing (NGS)

The integrity and quality of the extracted RNA samples were evaluated as following: 1% agarose gel electrophoresis to evaluate RNA degradation and possible contamination; Nanodrop (Life Technologies) to verify the purity of RNA (OD260/OD280); Qubit® 2.0 (Life Technologies) for quantification and the 2100 BioAnalyzer (Agilent) system for determination of RNA integrity (data not show). Subsequently the RNAs were stored in a chemically inert matrix GenTegra™ RNA (supplied by GenOne Biotechnologies) and sent for sequencing. The cDNAs were sequenced with the Illumina HiSeq 2500 platform. The sequences in FASTQ format were obtained from GenOne (<http://www.genone.com.br/>). Sequencing data has been deposited in BioProject (NCBI) database (<http://www.ncbi.nlm.nih.gov/bioproject/632590>) with accession number PRJNA632590.

2.3. Bioinformatics analyses for identification of miRNAs

Initially, the quality of the sequences was evaluated with the FastQC program, as previously described [18]. After the removal of the low-quality sequences with Trimmomatic program was performed [26]. The processed sequences were then mapped to the reference genome of *P. brasiliensis* present in NCBI (https://www.ncbi.nlm.nih.gov/genome/334?genome_assembly_id=212342) with the mapper.pl script of the mirDeep2 program [27]. The output mapping file was analyzed by the mirDeep2.pl script to search for pre-miRNA structures in the *P. brasiliensis* genome. With pre-microRNAs predicted, mirDeep2 outputs their sequences, including the predicted mature and star sequences in FASTA format. The FASTA file obtained through the mirDeep database was analyzed against the RNA fold database (<http://rna.tbi.univie.ac.at/cgi-bin/RNAWebSuite/RNAfold.cgi>) [28] in order to identify characteristics of pre-miRNAs such as hairpin, stem-loop and low values of minimum free energy (MFE). Through measurement of MFE it is possible to assess how robust is interaction of nitrogenous bases from pre-miRNA and consequently evaluate its base complementarity. These values are also used in the analysis of miRNA/target interaction. A good miRNA: mRNA binding is reflected by a small free energy, suggesting that the predicted binding is stable and true hybridization is likely to occur [28]. The threshold for acceptable MFE values varies, and here we adopt –20 kcal/mol [29].

2.4. miRNA differential expression analysis by RNA-Seq and prediction of target genes in *P. brasiliensis*

The expression of each miRNA in each sample was obtained by counting the number of reads mapped to each miRNA using the script `quantifier.pl` from miRDeep2, as previously described. The result was a counting matrix with each miRNA as rows and each library sample (iron-deprivation and control, with replicates) as columns. This count matrix was used for statistical tests of differential expression using a Negative Binomial GLM (Generalized Linear Model) with the R package DESeq2 [30], as previously described [18]. The miRNAs differential expression showed (p -value < 0.05 and False Discovery Rate (FDR) < 0.16).

To analyze potential gene targets of differentially expressed miRNA, we retrieved the 3' UTR and 5' UTR sequences from all the transcripts of *P. brasiliensis* downloaded from the NCBI database (https://www.ncbi.nlm.nih.gov/genome/334?genome_assembly_id=212342). The 3' UTR and 5' UTR sequences were obtained with a custom Perl script as the first and last 200 bp sequences from the entire transcripts. The RNAhybrid [31] was used to predict *P. brasiliensis* genes potentially targeted by the differentially expressed miRNA. The functional classification of the targets was performed through the Blast2GO and Funct2 programs [32].

2.5. Analysis of the expression of transcripts by quantitative real-time PCR (RT-qPCR) the expression of some targets of miRNAs was analyzed by RT-qPCR

The selected targets in *P. brasiliensis* include the glucose repression regulatory protein TUP1 (GenBankXP_010761638) and pH-response transcription factor `pacC/RIM101` (GenBankXP_010756067.1). Total RNA obtained from cells of *P. brasiliensis* cultivated in presence or iron deprivation during 24 h, were incubated with DNase (RQ1 RNase-free DNase, Promega) and subsequently subjected to in vitro reverse transcription (SuperScript III First-Strand Synthesis SuperMix; Invitrogen, Life Technologies), using Oligo (dT) for the annealing of the template-primer. Synthesized cDNAs were used in the RT-qPCR reaction using QuantStudio Real-Time PCR (ThermoFisher scientific) with a mixture of SYBR green PCR master mix (Applied Biosystems, Foster City, CA). The choice of gene for normalization was performed with Norm-Finder test [33] and the transcript coding for enolase (GenBankXP_010759701.1) was selected as the normalizer (Supplementary Table 1). For the experiment, standard curves were generated by a dilution of 1/5 of the cDNA and the relative expression levels of the transcripts were calculated using the standard curve method for relative quantification [34]. Statistical comparisons were performed using the Student's *t*-test and $p \leq 0.05$ values were considered statistically significant.

2.6. Mitochondrial activity and dosage of chitin in yeast cells

For labeling experiments, *P. brasiliensis* yeast cells cultivated in iron content and iron deprivation were collected at density of 10^6 cells/mL. To evaluate the effect of iron deprivation in mitochondria, cells were incubated with 400 μ M of MitoTracker Green FM (Sigma–Aldrich), and 2.4 μ M of Rhodamine 123 (Sigma–Aldrich) for 45 min at 37 °C in order to evaluate mitochondrial integrity and functionality, respectively. Levels of chitin were assessed after staining yeast cells with Calcofluor White (CFW, Sigma Biochemical) (100 μ g/mL in PBS) for 30 min and washing with PBS 1 X, twice. Posteriorly yeast cells were analyzed in a fluorescence microscope (Zeiss AxioCam MRC – Scope A1). The calculation of fluorescence intensity for both experiments was performed using the AxioVision Software (Carl Zeiss). Fifty cells in

each microscope slide, in triplicates were used. This software provides the intensity fluorescence in (pixels) and the standard error of each analysis. For statistical analysis Student's *t*-test was used and p -values ≤ 0.05 were considered statistically significant.

3. Results

3.1. Construction of miRNA libraries and identification of miRNAs

Libraries of miRNAs were constructed and the cDNAs were sequenced through the Illumina HiSeq2500 platform, with biological triplicates. The number of raw sequences ranged from 44, 257, 309 to 53,170,959 in the libraries. The sequence number data are depicted in (Supplementary Table 2). The total of sequences alignment from libraries in *P. brasiliensis* is demonstrated in Supplementary Table 2. In general, 100% of the reads were mapped to the reference genome.

After mapping in the genome of *P. brasiliensis*, the sequences were analyzed using the miRDeep2 program, to evaluate potential precursors and mature miRNAs; after this analysis, 45 miRNAs were identified among the analyzed libraries as shown in Table 1. Of special note, eight miRNAs were differentially expressed regarding the studied conditions. Five miRNAs were more abundant in iron deprivation (Fig. 1A–E) and three miRNAs demonstrated reduced abundance during iron deprivation (Fig. 1F–H). The value of the differential expression was calculated using p -value < 0.05 and FDR < 0.16 (Supplementary Table 3). The predicted structure of the sequences of eight miRNAs differentially expressed presented characteristics of staples, with minimum values of folding free energy (MFE) similar to miRNAs described in other microorganisms [35,36] as shown in Fig. 2.

3.2. Oxidative phosphorylation and response to oxidative stress are potentially regulated by miRNAs with increased abundance during iron deprivation

Due to the sequence complementarity in regions 3' and 5' UTR, it was possible to identify target genes of miRNA regulated during iron deprivation. Several metabolic processes can be regulated by differentially expressed miRNAs during iron deprivation, as following: general metabolism, biogenesis of cell wall components, transport of micronutrients, cells rescue, defense, and virulence (Supplementary Fig. 1). Among miRNAs with increased abundance in iron deprivation *PbFe*-miR 6, *PbFe*-miR 33 and *PbFe*-miR 42, probable regulate proteins involved with oxidative phosphorylation and oxidative stress response (Supplementary Table 4). To assess whether in fact the activity of the electron transport chain was compromised by iron deprivation for 24 h, yeast cells were stained with Rhodamine and analyzed by fluorescence microscopy, as shown in Fig. 3 A and C. Iron deprivation significantly reduced the mitochondrial activity. However, the integrity of mitochondrion is not affected by iron deprivation, as showed by staining with Mitotracker (Fig. 3A, B). In this work, proteins involved with cell rescue, defense and virulence such as Glutaredoxin (`PADG_00140`), Superoxide dismutase `Sod5` (`PADG_01954`) were also targets of miRNAs increased during iron deprivation (Supplementary Table 4). Therefore, we suggest that these pathways may be influenced by post-transcriptional regulation mediated by miRNAs.

3.3. Regulation of chitin synthesis and protein glycosylation by miRNAs

Metal deprivation imposed by the host, remodels various processes in fungi, including cell wall and glycosylation of proteins [37,38]. In this way, proteins involved with O and N-glycosylation

Table 1
miRNAs present in the libraries derived of small RNAs in yeast cells of *P. brasiliensis* in iron deprivation.

miRNAs	Mature Sequence	Star sequence	Precursor sequence	Genomic location
<i>PbFe_miR1</i>	TAAGACGCGAACTGTTGAGGT	TATCCAACGGTTCCTATTGGCGT	TAAGACGCGAACTGTTGAGGTTCGTAGAATTATCCAACGGTTCCTATTGGCGT	Supercontig_2.8_29838
<i>PbFe_miR2</i>	TGCTTTGGCTTCAAGATCTGC	TTGTACTTGCTGCCTGTGCTGC	CAGTTACAGTATCAGATTCACCTTGTGCTTGTGTTCTTTGAGAGTTCCTGCTGATAGAGA	Supercontig_2.5_20412
<i>PbFe_miR3</i>	TGAATGCTGTCATGAACCTGTC	CAGTTCAGTATCAGATTCAC	TCATCTATGAATGCTGTCATGAACCTGTC	Supercontig_2.16_40497
<i>PbFe_miR4</i>	TGAATGCTGTCATGAACCTGTC	TAATCAGTCCAGTATCAGA	TAATCAGTCCAGTATCAGATTCACCTCTGCTTGTATTCTTTGAGAGTCATGCTGTAGATTAG	Supercontig_2.20_42583
<i>PbFe_miR5</i>	TATGCTTGATCGGATTGAAGA	TAGATGTCATGAAGGCAAAAGGC	AAGATCATCTATGAATGCTGTCATGAACCTGTC	Supercontig_2.10_34794
<i>PbFe_miR6*</i>	TCAATTGAGGTGGCTGT	AGACACTATCAATCTTCCATG	TATGCTTGATCGGATTGAAGAAGACCTAGATGTCATGAAGGCAAAAGGC	Supercontig_2.12_38013
<i>PbFe_miR7</i>	TGGACTTGATATTGCAGTTTGT	TGAGTTCATCAAAATCCCTTT	AGACACTATCAATCTTCCATGTTAGAGCAACATATATTCTTCTATTGTATAGGGGCTATTCT	Supercontig_2.12_38022
<i>PbFe_miR8</i>	TATGGTAGAGGATTTTGTG	ACAGGGTGTTTTGTGTAAGA	CCTCTCTACTTGTGCTGCAGGGGCTCAATTGAGGTGGCTGT	Supercontig_2.9_33411
<i>PbFe_miR9–</i>	TAGACAGATGTGTTGATAGA	TATCCCATCAGCATGACT	TGAGTTCATCAAAATCCCTTTAGTGGACTTGATATTGCAGTTGT	Supercontig_2.12_37087
<i>PbFe_miR10–</i>	TAGACAGACATGTGGTATAGA	TATTAGAGTGTCTACTAGC	TATGCTTGATCGGATTGAAGAAGACCTAGATGTCATGAAGGCAAAAGGC	Supercontig_2.10_34411
<i>PbFe_miR11</i>	TATGTGCAGCATGTGGA	TGCATGAGCATGATTTGTGA	CCTCTCTACTTGTGCTGCAGGGGCTCAATTGAGGTGGCTGT	Supercontig_2.5_20505
<i>PbFe_miR12</i>	TAGGCCTAATCGGGCGCCGAGC	TCGGTCCGCGCTGAGCCTA	TGAGTTCATCAAAATCCCTTTAGTGGACTTGATATTGCAGTTGT	Supercontig_2.2_7137
<i>PbFe_miR13</i>	TTTCCCCTTTCTATTTTG	AAAAAGAGGAAGGGTGTAGAGGCGATC	TAGGCCTAATCGGGCGCCGAGCCTAATCCGACGTCGAGTCTAATTAGGGCGGGGCTC	Supercontig_2.6_26586
<i>PbFe_miR14</i>	TGAGACTGGGATTTACAT	TGAGAGACACCATAGGCCT	GGTCCGGCTCGGTCCGCGCTGAGCCTA	Supercontig_2.9_33031
<i>PbFe_miR15</i>	TGAGACTGGGATTTACAT	TGAGAGACACCATAGGCCT	AAAAAGAGGAAGGGTGTAGAGGCGATCAAAAGAACAACATGTTTGTCCCCTTTCTA	Supercontig_2.9_33019
<i>PbFe_miR16</i>	TATCTCGTTCTCTGAAT	TGGCCTCGAGAGGTAGTTCGG	TTTGT	Supercontig_2.6_24194
<i>PbFe_miR17</i>	TGTGGGGCGAGGCAGTAATTGT	TCAGCCAAGCTCTATAACAGT	TGAGACTGGGATTTACATATGGAATGCCTCTATGTAGTTGATTAATAGAGTGGCATG	Supercontig_2.25_44345
<i>PbFe_miR18</i>	TATCTGGTGAATATGAAGA	TGACTGATTCTAAGGGTGGTATCT	GAGACACCATAGGCCT	Supercontig_2.17_41190
<i>PbFe_miR19</i>	TATGATAGAGAATTTTGTGGC	TGAGAAGTTTACTGTCAGA	TGAGACTGGGATTTACATATGGAATGCCTCTATGTAGTTGATTAATAGAGTGGCATG	Supercontig_2.27_44987
<i>PbFe_miR20</i>	GTCAGTAAAGGATATGTATAGATT	ATTTACACACGACTTCTGACT	AGACACCATAGGCCT	Supercontig_2.14_39334
<i>PbFe_miR21</i>	ATAGGCCTCTGGCCCTAAGATTAC	CCTCTATATGAACCAGGGAATA	AGAGACCATAGGCCT	Supercontig_2.11_35831
<i>PbFe_miR22</i>	TTCTGGCTGTATGAGAGATGA	ATCTTTCTCAGCTCTAGTGATCA	AGAGACCATAGGCCT	Supercontig_2.1_948
<i>PbFe_miR23</i>	TGATGCTGTGCTCAATGCTGTGT	TGTTGAGTGTTCATTAGATGT	TATCTCGTTCTCTGAATCATTGGCCTCGAGAGGTAGTTCGG	Supercontig_2.19_41939
<i>PbFe_miR24</i>	TGATGCTGTGCTCAATGCTGTGT	TGTTGAGTGTTCATTAGATGT	TGTGGGGCGAGGCAGTAATTGTGTGACTGAAATGCTTAATCTTATACCAACATCAGCC	Supercontig_2.19_42152
<i>PbFe_miR25</i>	CCAGTCAGGGCTGAATCGGAGG	TCGTGCGCAGCCAAAAGCTGACC	AAGCTCTATAACAGT	Supercontig_2.7_27255
<i>PbFe_miR26</i>	TAATCCGACGTCGAGTCTAACCGG	TCAGTCGGGCGCTGAGCCTA	TATCTGGTGAATATGAAGATTTGACAGCCGTGAACCTAGGTTCTAGAGGAAGAAATTTG	Supercontig_2.22_43403
<i>PbFe_miR27–</i>	CTGGACGTCGGATTAAGCTCGT	GAGCCCCACCGAGGCCCCCGTT	ACTGATTCTAAGGGTGGTATCT	Supercontig_2.19_42075
<i>PbFe_miR28</i>	TAGTTAGGTTAGTTAGTTA	ACTAAGTTAGTTAACAGTTAAC	ACTGATTCTAAGGGTGGTATCT	Supercontig_2.4_17303
<i>PbFe_miR29</i>	TTCTTTATGAACAGTGGCTGGT	CAGTCAITCATTGAGAATT	TATGATAGAGAATTTTGTGGCTGAGATGCAGTGAAGTTTACTGTCAGA	Supercontig_2.2_8400
<i>PbFe_miR30*</i>	TAGGAGCTCTGCATCATTGTC	TTGCTAGTGTTTTGTGCA	GTCAGTGAAGGATATGTATAGATTGAAATGTATTTACACACGACTTCTGACT	Supercontig_2.9_32563
<i>PbFe_miR31</i>	TAATGCTGTGCTGATGCT	TGCATTAGATTTGGGTTGG	ATAGGCCTCTGGCCCTAAGATTACATCTCGGATGAGCACAAGCGCACCTAGGCA	Supercontig_2.19_42259
<i>PbFe_miR32</i>	TTGTGGAGATCTAGAGTTCTT	TCTCTTTTCTACATTGACTT	TCCTCTATATGAACCAGGGAATA	Supercontig_2.9_33308
<i>PbFe_miR33*</i>	TGAGATTTCTGTCCCTCAGT	TGCTAGTCAATCAGATCATG	TCCTGGCTGTATGAGAGATGACTTATTATCTTCTCAGCTCTAGTGATCA	Supercontig_2.21_43052
<i>PbFe_miR34</i>	TGCCAGAGTCAGAGTGTGGTGA	ATTGTGCAGGCTGACTTGGCCACA	TGTTGAGTGTTCATTAGATGT	Supercontig_2.9_33531

PbFe_mir35	TATCAGACTGTCGTTTTAAGGAAT	TCTTGCATAAACGACAGTCCCTCGCATGAT	TCTTGCATAAACGACAGTCCCTCGCATGAT	Supercontig.2.4_19368
PbFe_mir36	TGTCACATTATCTCTTTGAGCTTCAITCA	GAAAGCTTCAITGTCATITCA	TGTCACATTATCTCTTTGAGCTTCAITCA	Supercontig.2.14_39362
PbFe_mir37	TAAAGCTGACAGAAITGACACC	TGTCGGCAACAGTTTTTATC	TGTCGGCAACAGTTTTTATC	Supercontig.2.8_29683
PbFe_mir38	TCTGGTACAGTAGTAAGGGGG	CTCTTGATCTTTTCAGAGG	CTCTTGATCTTTTCAGAGGTTGAAAGT	Supercontig.2.29_45462
PbFe_mir39	ATTCTCTGTGAGCTCAGTGA	TTTCTTCTTCCAGTACTAG	ATTCTCTGTGAGCTCAGTGAITATCT	Supercontig.2.20_42660
PbFe_mir40	TATTCTGTATAGAACACTGTTTCTT	TGGTCTGTGAGACTGATCTGA	TGGTCTGTGAGACTGATCTGAAGACT	Supercontig.2.9_33339
PbFe_mir41*	TATTCTATTATGCTGTTTA	CACAGACAGAAITCAGAITGAA	CACAGACAGAAITCAGAITGAA	Supercontig.2.21_43281
PbFe_mir42*	TTTCTGTAGTCTCTTTGGT	CGGAAGCCACAAAGG	TTTCTGTAGTCTCTTTGGTATGATAG	Supercontig.2.7_26996
PbFe_mir43	TTAGAATCTCTGACCCAGT	TGGACCTTAGAGTTCTGACCTGT	TTAGAATCTCTGACCCAGTCTCCAG	Supercontig.2.1_4199
PbFe_mir44	CTAGTTAGGTTAGTTAGTTA	GCTAACTAACTAACTAAAT	GCTAACTAACTAACTAACTAACTAACT	Supercontig.2.27_45070
PbFe_mir45	TATGGTAGAGGATTTTGTGCC	CACAGACTTTTCTGCTGAA	TATGGTAGAGGATTTTGTGCCAGATG	Supercontig.2.27_45057

(*) up-regulated miRNAs. (-) down-regulated miRNAs.

such as oligosaccharyltransferases (PADG_07841, PADG_05028), N-glycosyl-transferase (PADG_04497), dolichyl-diphosphooligosaccharide (PADG_03106) or involved with the GPI anchor synthesis as TED1 (PADG_04448) were putative targets of miRNAs increased during iron deprivation. In addition, proteins involved with chitin synthesis such as chitin synthase activator (PADG_05937), chitin synthase (PADG_02079), were also regulated by miRNAs increased in iron deprivation (Supplementary Table 5). The dosage of chitin at 24 h of iron deprivation (Fig. 4A, B), indicates the reduction of this polymer.

3.4. MiRNAs downregulated during iron deprivation potentially control the expression of transcriptional factors related to iron homeostasis

In this work, several miRNAs had as targets, transcriptional factors. MiRNAs with increased abundance in presence of iron such as PbFe-miR10 and PbFe-miR27, had as predicted targets the transcriptional factors *Tup1* and *pacC/Rim101*, respectively (Supplementary Table 6). Interestingly, these genes/transcription factors regulate the expression of various proteins involved with iron uptake [39,40]. For evaluation of the expression of these two genes RT-qPCR was performed. After 24 h of deprivation both genes depicted increased expression in iron deprivation (Fig. 5).

4. Discussion

In this work microRNA libraries, were obtained during growth of *P. brasiliensis* yeast cells in the presence and absence of iron. Bioinformatics analysis allowed an average of 45,309,202 reads mapped to the *P. brasiliensis* genome. The number of reads obtained and mapped to the *P. brasiliensis* genome is within the range found in other studies focusing on the characterization of miRNAs in fungi. For obtaining targets regulated by differentially expressed miRNAs during iron deprivation, analysis was performed in 3' and 5' UTRs. Several studies have already demonstrated the interaction of the miRNAs with both regions of mRNA [41]. In this way, this analysis allowed a better approach to the potential biological processes regulated by miRNAs in response the iron deprivation.

Metal deprivation is a mechanism developed by host, to decrease the growth of pathogenic microorganism during infection, and in contrast pathogens developed mechanisms of iron, zinc and copper uptake from the host to support growth in micronutrients scarcity [42]. *P. brasiliensis* presented microRNAs presumed to regulate oxidative phosphorylation during iron limitation as shown in Supplementary Table 4. Several members of the electron transport chain and of the ATP synthesis were here presumed to be down regulated by microRNAs during iron deprivation. This finding is remarkably interesting since analysis of proteomic responses of members of the *Paracoccidioides* genus during iron deprivation, revealed reprogrammed metabolic pathways, possible enabling the fungus to adapt an environment with limited metal [10]. Of the adaptive processes include the repression of oxidative phosphorylation [42].

Many proteins belonging to this metabolic pathway are dependent on iron and, under the limitation of this micronutrient, pathways such as glycolysis are preferably used to obtain energy during the limitation of this metal [10]. Similar results were described for *Cryptococcus neoformans* [43], *E. coli* [21] and *P. aeruginosa* [22], in which the iron deprivation reduced the activity of that metabolic pathway. In this way it is noteworthy the description of proteins related to oxidative phosphorylation and ATP synthesis regulated by microRNAs (Supplementary Table 4).

Data of decreased mitochondrial respiratory activity, as demonstrated by immunofluorescence (Fig. 3), reinforced

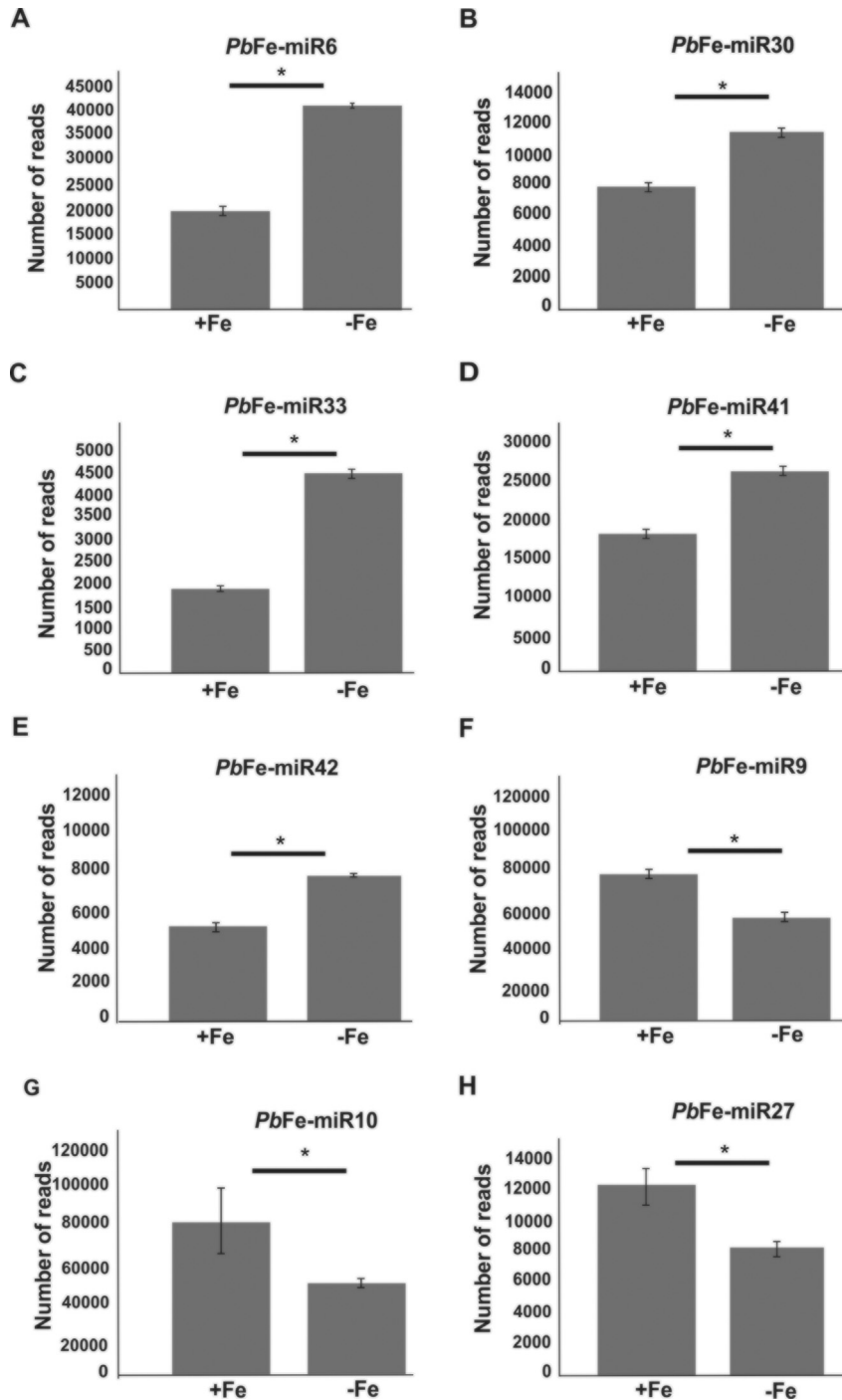


Figure 1. Expression profile of differentially regulated miRNAs during iron deprivation. (A–E). MiRNAs with increased abundance during iron deprivation. (F–H) MiRNAs with reduced expression during iron deprivation. The R package DESeq2 was used for differential expression analysis.

transcriptional analysis. Additionally, the decrease of oxidative phosphorylation, reduces the amount of reactive oxygen species within the cell [10] and therefore proteins involved in this response, were putatively down-regulated by microRNAs during iron deprivation (Supplementary Table 4).

During the development of fungal infections the cell wall is the first structure that interacts with host cells; proteins as well as carbohydrates present in this structure are essential for the development of infection as well as to elicit the host's immune responses [44]. *Paracoccidioides* spp. during infection in

macrophages [45] or in conditions of metal deprivation [38,46] change the constitution of the polymers present in the cell wall, as an adaptive response to colonization in different cells or tissues of the host. Proteins involved in chitin synthesis were here described as miRNA targets. Chitin synthase activator and chitin synthase involved in the production of this polymer were targets of miRNAs with higher abundance in iron deprivation. In complex fungi the amount of chitin and glucans are altered in yeast cells during colonization of the host where beta glucan is replaced by alpha glucan, a less immunogenic molecule [44]. During zinc deprivation

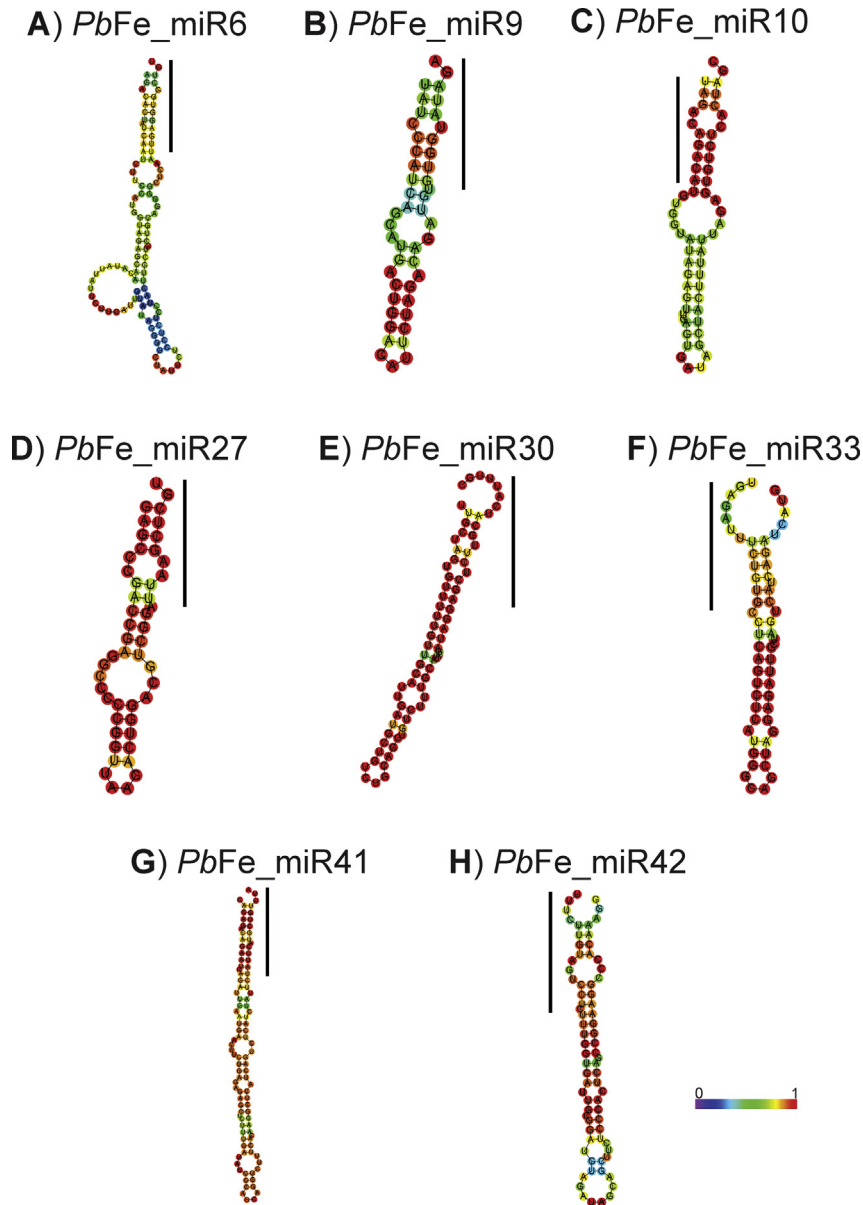


Figure 2. Structure of mi RNAs differentially expressed in iron deprivation. (A–H) Structure of the 8 miRNAs differentially regulated by iron deprivation. The mature miRNA portion is highlighted in black bar. The structures were generated using the Rfold program. The structures are colored according to the base pairing probabilities. The number 1 on the scale represents the probability of pairing between bases within the molecule. For example, *PbFe_miR6* and *miR9* have 63% and 68% probability, respectively of pairing between complementary bases. Red color denotes high probability pairing as seen in the bar scale.

in *P. brasiliensis* chitin synthesis is reduced [38]. Iron limitation in *Candida albicans* also reduces the amount of polymers in the cell wall, as demonstrated by fluorescent micrographs [37]. In this way, we suggest that miRNAs could respond to iron deprivation, acting on the cell wall polymer biosynthesis pathways (Supplementary Table 5 and Fig. 4), contributing to the adaptive responses of this fungus during micronutrient limitation.

Several proteins involved in glycosylation events were predicted targets of miRNAs with higher abundance during iron deprivation (Supplementary Table 5). In *P. lutzii* zinc deprivation reduces protein glycosylation [38]. In *C. albicans* the activity of α -1,2-mannosyltransferase is dependent on the concentration of iron [47], since oligosaccharyl transferases involved in glycosylation at early stages in the endoplasmic reticulum, present metals as Mn²⁺ and Fe²⁺, as cofactors [48].

In fungi of the genus *Paracoccidioides* the acquisition of iron occurs through production of siderophores, reductive iron acquisition and heme uptake [11,12,49]. In fungi, the control of the expression of iron uptake systems involves the expression of transcriptional factors that act by positively or negatively regulating the expression of genes according to the availability of metal [2,40]. Transcriptional factors have also been characterized as targets for miRNAs in several studies [50] including studies on fungi for example, in *Trichophyton rubrum* differentially expressed miRNAs during the mycelium and conidial stages, presented as targets the bZIP transcription factor, C6 transcription factor and TFIIB transcription factor [36]. In this work, the pH-response transcription factor *pacC/Rim101* was described as target of *PbFe_miR27*. In *C. albicans* the expression of the ferric reductases *Fre2p* and *Frp1p*, is controlled by *Rim 101*, in response to alkaline pH, and iron

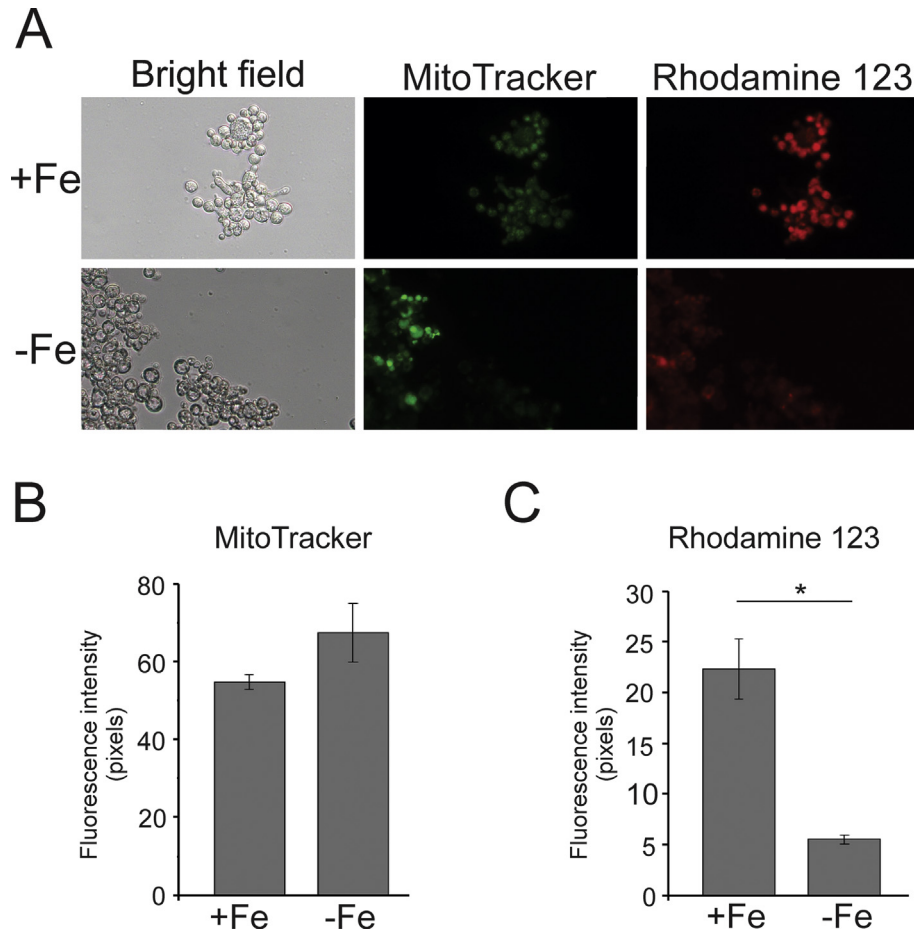


Figure 3. Mitochondrial activity of cells of *P. brasiliensis* under iron deprivation. (A) Yeast cells grown in 3.5 μM of $\text{Fe}(\text{NH}_4)_2(\text{SO}_4)_2$ (control), or 50 μM of BPS (deprivation) for 24 h, were stained with MitoTracker and Rhodamine 123. Digital images acquired using Axio-Scope A1 microscope. All images from light and fluorescence microscopy were obtained in magnification of 400 \times . (B) The MitoTracker fluorescence intensity. (C) The Rhodamine 123 fluorescence intensity. The fluorescence intensity was measured using the AxioVision software (Carl Zeiss, Germany). The values of fluorescence intensity (in pixels) and the standard deviation of each analysis were used to plot the graph. Data expressed as mean \pm standard deviation (error bars) of the minimum of 50 cells for each microscope slide, in triplicate, for each condition. ** indicates significant difference between the two conditions, the p -value ≤ 0.05 . The fluorescence intensity of the MitoTracker analysis was not significant between conditions.

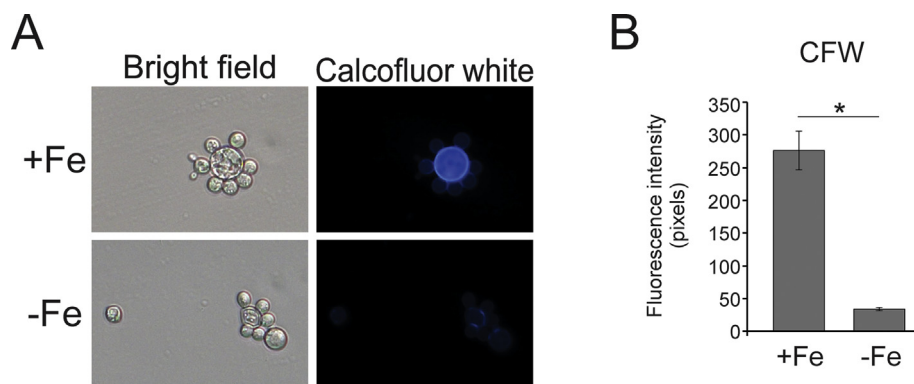


Figure 4. Dosage of chitin in *P. brasiliensis* cell wall in iron deprivation. (A) The yeast cells were incubated in the presence (3.5 μM of $\text{Fe}(\text{NH}_4)_2(\text{SO}_4)_2$) or iron deprivation (50 μM of BPS), during 24 h, and cell wall was stained with Calcofluor white (CFW). Digital images acquired using Axio-Scope A1 microscope. All images from light and fluorescence microscopy were obtained in magnification of 400. (B) The fluorescence intensity was measured using the AxioVision software (Carl Zeiss, Germany). The values of fluorescence intensity (in pixels) and the standard deviation of each analysis were used to plot the graph. Data expressed as mean \pm standard deviation (error bars) of the minimum of 50 cells for each microscope slide, in triplicate, for each condition. ** indicates significant difference between the two conditions, the p -value ≤ 0.05 .

deprivation [40]. As demonstrated by gene expression analysis, *pacC/Rim 101* is induced in iron deprivation and in contrast the *PbFe_miR27* is down-regulated in the same condition; therefore the increase of expression of *pacC/Rim 101*, could be due to

decreased expression of this miRNA, that potentially regulate post-transcriptionally this gene.

Another transcriptional factor involved in response to iron deprivation is called Tup1; in *C. neoformans* this transcriptional

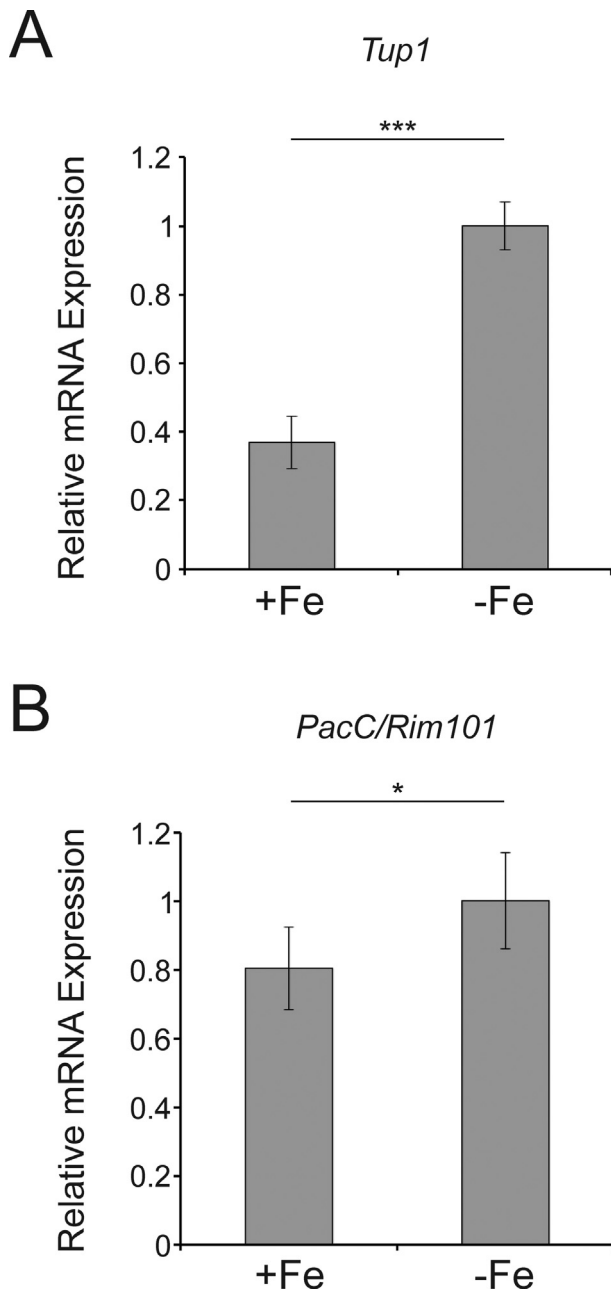


Figure 5. Expression of potential targets of miRNAs regulated in iron deprivation. Experiments performed by real-time RT-PCR in yeast cells of *Paracoccidioides brasiliensis*, incubated in presence of 3.5 μ M ferrous sulphate or in iron deprivation by addition of 50 μ M BPS. Expression of *Tup1* (GenBankXP_010761638) and pH-response transcription factor *pacC/Rim101* (GenBankXP_XP_010756067.1) after 24 h of iron deprivation. Data were normalized with the transcript encoding the enolase protein (GenBankXP_010759701.1). The Student's t-test was used for statistical comparisons. Error bars represent the standard deviation of three biological replicates. (*) $p \leq 0.05$ and (***) $p \leq 0.0005$.

factor controls several processes such as melanin synthesis and metal uptake. In this fungus, knockout mutant strains for *Tup1*, in iron deprivation, present a decrease in the expression of genes involved in high-affinity iron and copper uptake systems [39]. Therefore, in an environment where iron is available, the expression of this factor is not necessary, since this gene controls proteins involved in the high affinity iron uptake pathway, and in this sense the expression of *Tup1* is repressed in the presence of iron, and potentially *PbFe_miR10*, acts during this regulation.

In general, we demonstrated that miRNAs produced by *P. brasiliensis* are regulated by the availability of iron and such molecules may regulate metabolic pathways that contribute to the fungus' adaptation to a limited iron environment. In this sense, miRNA with higher abundance during iron deprivation, may act on oxidative phosphorylation, synthesis of cell wall polymers and in protein glycosylation events. In contrast, miRNAs with higher abundance in the presence of iron may regulate transcription factors that regulate the expression of genes involved in high affinity iron uptake pathways.

Declaration of competing interest

The authors have no conflict of interest to declare.

Acknowledgments

This work at Universidade Federal de Goiás was supported by grants from Fundação de Amparo a Pesquisa do Estado de Goiás (FAPEG), INCT. CMAS is a fellow from Conselho Nacional de Desenvolvimento Científico e Tecnológico (CNPq). The authors want to thank Juliano D Pancez for the helpful suggestions and assistance.

Appendix A. Supplementary data

Supplementary data to this article can be found online at <https://doi.org/10.1016/j.micinf.2020.10.008>.

References

- [1] Zhang V, Nemeth E, Kim A. Iron in lung pathology. *Pharmaceuticals* 2019;12: 1–11. <https://doi.org/10.3390/ph12010030>.
- [2] Ganz T. Iron and infection. *Int J Hematol* 2018;107:7–15. <https://doi.org/10.1007/s12185-017-2366-2>.
- [3] Stocks CJ, von Pein JB, Curson JEB, Rae J, Phan MD, Foo D, et al. Frontline Science: LPS-inducible SLC30A1 drives human macrophage-mediated zinc toxicity against intracellular *Escherichia coli*. *J Leukoc Biol* 2020;1–11. <https://doi.org/10.1002/JLB.2HI0420-160R>.
- [4] Lonergan ZR, Skaar EP. Nutrient zinc at the host–pathogen interface. *Trends Biochem Sci* 2019;44:1041–56. <https://doi.org/10.1016/j.tibs.2019.06.010>.
- [5] Horianopoulos LC, Kronstad JW. Connecting iron regulation and mitochondrial function in *Cryptococcus neoformans*. *Curr Opin Microbiol* 2019;52:7–13. <https://doi.org/10.1016/j.mib.2019.04.002>.
- [6] Gupta M, Outten CE. Iron–sulfur cluster signaling: the common thread in fungal iron regulation. *Curr Opin Chem Biol* 2020;55:189–201. <https://doi.org/10.1016/j.cbpa.2020.02.008>.
- [7] Kurucz V, Krüger T, Antal K, Dietl AM, Haas H, Pócsi I, et al. Additional oxidative stress reroutes the global response of *Aspergillus fumigatus* to iron depletion. *BMC Genom* 2018;19:1–19. <https://doi.org/10.1186/s12864-018-4730-x>.
- [8] Shikanai-Yasuda MA, Mendes RP, Colombo AL, de Queiroz-Telles F, Kono ASG, Paniago AMM, et al. Brazilian guidelines for the clinical management of paracoccidioidomycosis. *Rev Soc Bras Med Trop* 2017;50:715–40. <https://doi.org/10.1590/0037-8682-0230-2017>.
- [9] Silva MG, Schrank A, Bailão EFLC, Bailão AM, Borges CL, Staats CC, et al. The homeostasis of iron, copper, and zinc in *Paracoccidioides brasiliensis*, *Cryptococcus neoformans* var. *Grubii*, and *Cryptococcus gattii*: a comparative analysis. *Front Microbiol* 2011;2:1–19. <https://doi.org/10.3389/fmicb.2011.00049>.
- [10] Parente AFA, Bailão AM, Borges CL, Parente JA, Magalhães AD, Ricart CAO, et al. Proteomic analysis reveals that iron availability alters the metabolic status of the pathogenic fungus *Paracoccidioides brasiliensis*. *PLoS One* 2011;6. <https://doi.org/10.1371/journal.pone.0022810>.
- [11] Silva MG, De Curcio JS, Silva-Bailão MG, Lima RM, Tomazett MV, de Souza AF, et al. Molecular characterization of siderophore biosynthesis in *Paracoccidioides brasiliensis*. *IMA Fungus* 2020;11. <https://doi.org/10.1186/s43008-020-00035-x>.
- [12] Bailão EFLC, Parente JA, Pigosso LL, de Castro KP, Fonseca FL, Silva-Bailão MG, et al. Hemoglobin uptake by *Paracoccidioides* spp. is receptor-mediated. *PLoS Negl Trop Dis* 2014;8. <https://doi.org/10.1371/journal.pntd.0002856>.
- [13] Bailão EFLC, Lima P de S, Silva-Bailão MG, Bailão AM, Fernandes G da R, Kosman DJ, et al. *Paracoccidioides* spp. ferrous and ferric iron assimilation pathways. *Front Microbiol* 2015;6:1–12. <https://doi.org/10.3389/fmicb.2015.00821>.

- [14] de Curcio JS, Batista MP, Pაცეც JD, Novaes E, Soares CM de A. In silico characterization of microRNAs-like sequences in the genome of *Paracoccidioides brasiliensis*. *Genet Mol Biol* 2019;42:95–107. <https://doi.org/10.1590/1678-4685-gmb-2018-0014>.
- [15] Matsuyama H, Suzuki HI. Systems and synthetic microRNA biology: from biogenesis to disease pathogenesis. *Int J Mol Sci* 2020;21:1–23. <https://doi.org/10.3390/ijms21010132>.
- [16] Singulani J, Da Silva J, Gullo F, Costa M, Fusco-Almeida AM, Enguita F, et al. Preliminary evaluation of circulating microRNAs as potential biomarkers in paracoccidioidomycosis. *Biomed Rep* 2017;3:53–7. <https://doi.org/10.3892/br.2017.849>.
- [17] Loh HY, Norman BP, Lai KS, Rahman NMANA, Alitheen NBM, Osman MA. The regulatory role of microRNAs in breast cancer. *Int J Mol Sci* 2019;20:1–27. <https://doi.org/10.3390/ijms20194940>.
- [18] De Curcio JS, Pაცეც JD, Novaes E, Brock M, De Almeida Soares CM. Cell wall synthesis, development of hyphae and metabolic pathways are processes potentially regulated by microRNAs produced between the morphological stages of *Paracoccidioides brasiliensis*. *Front Microbiol* 2018;9. <https://doi.org/10.3389/fmicb.2018.03057>.
- [19] Paul S, Datta SK, Datta K. miRNA regulation of nutrient homeostasis in plants. *Front Plant Sci* 2015;6:1–11. <https://doi.org/10.3389/fpls.2015.00232>.
- [20] Davis M, Clarke S. Influence of microRNA on the maintenance of human iron metabolism. *Nutrients* 2013;5:2611–28. <https://doi.org/10.3390/nu5072611>.
- [21] Masse Eric, Carin K, Vanderpool SG. Effect of RyhB small RNA on global iron use in *Escherichia coli*, vol. 187; 2005. p. 3–10. <https://doi.org/10.1128/JB.187.20.6962>.
- [22] Nelson CE, Huang W, Brewer LK, Nguyen AT, Kane MA, Wilks A, et al. Proteomic analysis of the *Pseudomonas aeruginosa* iron starvation response reveals PrrF small regulatory RNA-dependent iron regulation of Twitching motility, amino acid metabolism, and zinc homeostasis proteins. *J Bacteriol* 2019;201:1–23. <https://doi.org/10.1128/JB.00754-18>.
- [23] Zhang L, Ye Y, Tu H, Hildebrandt MA, Zhao L, Heymach JV, et al. MicroRNA-related genetic variants in iron regulatory genes, dietary iron intake, microRNAs and lung cancer risk. *Ann Oncol Off J Eur Soc Med Oncol* 2017;28:1124–9. <https://doi.org/10.1093/annonc/mdx046>.
- [24] Fava-Netto C. Estudos quantitativos sobre fixação de complemento na blastomicose sul americana, com antígeno polissacarídico. *Arq Cir Clin* 1955;18:97–254.
- [25] Restrepo AJB. Growth of *Paracoccidioides brasiliensis* yeast phase in a chemically defined culture medium. *J Clin Microbiol* 1980;12:279–81.
- [26] Bolger AM, Lohse M, Usadel B. Trimmomatic: a flexible trimmer for Illumina sequence data. *Bioinformatics* 2014;30:2114–20. <https://doi.org/10.1093/bioinformatics/btu170>.
- [27] Friedländer MR, MacKowiak SD, Li N, Chen W, Rajewsky N. MiRDeep2 accurately identifies known and hundreds of novel microRNA genes in seven animal clades. *Nucleic Acids Res* 2012;40:37–52. <https://doi.org/10.1093/nar/gkr688>.
- [28] Lorenz R, Wolfinger MT, Tanzer A, Hofacker IL. Predicting RNA secondary structures from sequence and probing data. *Methods* 2016;103:86–98. <https://doi.org/10.1016/j.ymeth.2016.04.004>.
- [29] Trotta E. On the normalization of the minimum free energy of RNAs by sequence length. *PLoS One* 2014;9. <https://doi.org/10.1371/journal.pone.0113380>.
- [30] Anders S, Huber W. Differential expression analysis for sequence count data. *Genome Biol* 2010;11. <https://doi.org/10.1186/gb-2010-11-10-r106>.
- [31] Rehmsmeier M, Steffen P, Hochsmann M, Giegerich R. Fast and effective prediction of microRNA/target duplexes. *RNA* 2004;10:1507–17. <https://doi.org/10.1261/rna.5248604>.
- [32] Conesa A, Götz S, García-Gómez JM, Terol J, Talón M, Robles M. Blast2GO: a universal tool for annotation, visualization and analysis in functional genomics research. *Bioinformatics* 2005;21:3674–6. <https://doi.org/10.1093/bioinformatics/bti610>.
- [33] Andersen CL, Jensen JL, Ørntoft TF. Normalization of real-time quantitative reverse transcription-PCR data: a model-based variance estimation approach to identify genes suited for normalization, applied to bladder and colon cancer data sets. *Cancer Res* 2004;64:5245–50. <https://doi.org/10.1158/0008-5472.CAN-04-0496>.
- [34] Bookout AL, Cummins CL, Kramer MF, Pesola JM, Mangelsdorf D J, Mangelsdorf DJ, et al. High-throughput real-time quantitative reverse transcription PCR, vol. Chapter 15; 2006. <https://doi.org/10.1002/0471142727.mb1508s73>.
- [35] Chen R, Jiang N, Jiang Q, Sun X, Wang Y, Zhang H, et al. Exploring microRNA-like small RNAs in the filamentous fungus *Fusarium oxysporum*. *PLoS One* 2014;9:e104956. <https://doi.org/10.1371/journal.pone.0104956>.
- [36] Wang L, Xu X, Yang J, Chen L, Liu B, Liu T, et al. Integrated microRNA and mRNA analysis in the pathogenic filamentous fungus *Trichophyton rubrum*. *BMC Genom* 2018;19:1–14. <https://doi.org/10.1186/s12864-018-5316-3>.
- [37] Tripathi A, Liverani E, Tsygankov A, Puri S. Iron alters the cell wall composition and intracellular lactate to affect *Candida albicans* susceptibility to antifungals and host immune response. *J Biol Chem* 2020. <https://doi.org/10.1074/jbc.ra120.013413>.
- [38] De Curcio JS, Silva MG, Silva Bailão MG, Bão SN, Casaletti L, Bailão AM, et al. Identification of membrane proteome of *Paracoccidioides lutzii* and its regulation by zinc. *Futur Sci OA* 2017;3. <https://doi.org/10.4155/fsoa-2017-0044>.
- [39] Lee H, Chang YC, Varma A, Kwon-Chung KJ. Regulatory diversity of TUP1 in *Cryptococcus neoformans*. *Eukaryot Cell* 2009;8:1901–8. <https://doi.org/10.1128/EC.00256-09>.
- [40] Baek YU, Li M, Davis DA. *Candida albicans* ferric reductases are differentially regulated in response to distinct forms of iron limitation by the Rim101 and CBF transcription factors. *Eukaryot Cell* 2008;7:1168–79. <https://doi.org/10.1128/EC.00108-08>.
- [41] Liu H, Bi J, Dong W, Yang M, Shi J, Jiang N, et al. Invasion-related circular RNA circFNDC3B inhibits bladder cancer progression through the miR-1178-3p/G3BP2/SRC/FAK axis. *Mol Cancer* 2018;17:1–19. <https://doi.org/10.1186/s12943-018-0908-8>.
- [42] Bairwa G, Hee Jung W, Kronstad JW. Iron acquisition in fungal pathogens of humans. *Metallomics* 2017;9:215–27. <https://doi.org/10.1039/c6mt00301j>.
- [43] Jung WH, Saikia S, Hu G, Wang J, Fung CKY, D'Souza C, et al. HapX positively and negatively regulates the transcriptional response to iron deprivation in *Cryptococcus neoformans*. *PLoS Pathog* 2010;6. <https://doi.org/10.1371/journal.ppat.1001209>.
- [44] Puccia R, Vallejo MC, Matsuo AL, Longo LVG. The *Paracoccidioides* cell wall: past and present layers toward understanding interaction with the host. *Front Microbiol* 2011;2:1–7. <https://doi.org/10.3389/fmicb.2011.00257>.
- [45] Chaves EGA, Parente-Rocha JA, Baeza LC, Araújo DS, Borges CL, Oliveira MAP de, et al. Proteomic analysis of *Paracoccidioides brasiliensis* during infection of alveolar macrophages primed or not by interferon-gamma. *Front Microbiol* 2019;10:1–14. <https://doi.org/10.3389/fmicb.2019.00096>.
- [46] Petito G, De Curcio JS, Pereira M, Bailão AM, Pაცეც JD, de Moraes COB, et al. Metabolic adaptation of *Paracoccidioides brasiliensis* in response to in vitro copper deprivation. *Front Microbiol* 2020;11:1834. <https://doi.org/10.3389/fmicb.2020.01834>.
- [47] Bai C, Xu X, Chan F, Teck R, Lee H, Wang Y. Encodes an iron-regulated α -1,2-Mannosyltransferase important for protein glycosylation, cell wall integrity, morphogenesis, and virulence in. *Society* 2006;5:238–47. <https://doi.org/10.1128/EC.5.2.238>.
- [48] Hendrickson TL, Imperiali B. Metal ion dependence of oligosaccharyl transferase: implications for catalysis. *Biochemistry* 1995;34:9444–50. <https://doi.org/10.1021/bi00029a020>.
- [49] Silva-Bailão MG, Bailão EFLC, Lechner BE, Gauthier GM, Lindner H, Bailão AM, et al. Hydroxamate production as a high affinity iron acquisition mechanism in *Paracoccidioides* Spp. *PLoS One* 2014;9. <https://doi.org/10.1371/journal.pone.0105805>.
- [50] Zhou Y, Ferguson J, Chang JT, Kluger Y. Inter- and intra-combinatorial regulation by transcription factors and microRNAs. *BMC Genom* 2007;8:1–10. <https://doi.org/10.1186/1471-2164-8-396>.